Available online at www.sciencedirect.com
ScienceDirect
Polymer 49 (2008) 1892–1901
polymer
www.elsevier.com/locate/polymer

Viscoelasticity of randomly crosslinked EPDM networks

G. Martin [a], C. Barrès [b,c,*], P. Cassagnau [a], P. Sonntag [d], N. Garois [d]

[a] Université Lyon 1, IMP/LMPB Laboratoire des Matériaux Polymères et Biomatériaux, Villeurbanne F-69622, France
[b] INSA-Lyon, IMP/LMM Laboratoire des Matériaux Macromoléculaires, Villeurbanne F-69621, France
[c] CNRS, UMR5223, Ingénierie des Matériaux Polymères, Villeurbanne F-69621, France
[d] Hutchinson S.A., Centre de Recherches, Rue Gustave Nourry, BP 31, F-45120 Chalette-sur-Loing, France

Received 7 December 2007; received in revised form 1 February 2008; accepted 5 February 2008
Available online 8 February 2008

Abstract

The network structure of plasticized EPDM compounds, crosslinked with resol at different concentrations, was studied by means of rheological methods consisting in oscillatory shear tests, to determine the equilibrium modulus G_e, and long-time relaxation tests in compression followed by strain recovery (a protocol that also yielded values of the compression set of the samples). G_e results were analyzed with respect to the phenomenological model of Langley and Graessley which takes into account the contribution of crosslinks and trapped entanglements to the shear equilibrium modulus. A correction was introduced in order to take into account the presence of plasticizer. The measurement of the soluble polymer fraction in the different samples allowed a more detailed characterization of the networks to be carried out, following a molecular approach by Pearson and Graessley. This method enabled to calculate the crosslink density and trapping factor, but also to compute the probability ψ_1 for an un-crosslinked polymer unit to belong to a dangling chain. This probability was shown to increase as resol concentration, and then crosslink density, decreased. The empirical Chasset–Thirion equation was used to model the long-time relaxation data for each sample. Chasset–Thirion parameters were interpreted by Curro and Pincus within a theoretical framework based on the idea that the longest relaxation times are associated with the pendent chains of the network. The relaxation times, obtained from the fitting of experimental relaxation moduli, dramatically increased as the crosslink density decreased. This result corroborates the evolution of ψ_1: both tend to demonstrate that in the present compounds, the decrease of crosslink density is accompanied by an increase of the number and length of the dangling chains, leading to increasing relaxation times. The large soluble fraction and long pendent chains of samples showing the lowest crosslink densities were responsible for their poor elastic recovery. The relaxation data were used to model the elastic recovery of the compounds and predict their compression set profiles. Very satisfactory agreement was obtained between experimental data and computations.

Keywords: EPDM networks; Viscoelastic properties; Dangling chains

1. Introduction

Ethylene–propylene–diene (EPDM) terpolymers are elastomeric materials which combine a saturated polymer backbone with residual unsaturations as side groups. As a consequence, they are more resistant to oxygen, ozone, UV and heat than commodity polydiene elastomers. Their resistance to swelling in apolar fluids, such as oil, is, however, poor. The diene monomers used in commercial EPDM terpolymers are very few: 5-ethylidene-2-norbornene (ENB), dicyclopentadiene and 5-vinylidene-2-norbornene are currently the only ones. Most EPDM applications require its crosslinking. This is achieved by using mainly three types of crosslinking agents: sulfur, peroxides and alkylphenol–formaldehyde resins (resols). Peroxide is gradually gaining importance at the expense of sulfur, essentially because of the high thermal stability of the C–C intermolecular bonds formed in co-agent-assisted peroxide crosslinking of EPDMs. This matches the growing high-temperature demand of end-users. Resols also provide high-temperature stability and are employed preferentially in thermoplastic vulcanizates (TPVs), which generally comprise a polypropylene phase which would deteriorate if peroxides were used.

* Corresponding author. INSA-Lyon, IMP/LMM Laboratoire des Matériaux Macromoléculaires, Villeurbanne, F-69621, France.
E-mail address: claire.barres@insa-lyon.fr (C. Barrès).

0032-3861/$ - see front matter © 2008 Elsevier Ltd. All rights reserved.
doi:10.1016/j.polymer.2008.02.003

The mechanisms of the different reaction schemes implemented for EPDM crosslinking have been derived from studies either aimed at modeling the rubber crosslinking chemistry by use of low molar weight model olefins or at direct analysis of the crosslinked material. However, due to the low unsaturation content of EPDM, the use of spectroscopic techniques initially suffered from analytical sensitivity problems. These were overcome with technological evolutions, allowing infrared and solid state NMR spectroscopies to become the main direct analytical techniques for crosslinked elastomers. For instance, infrared spectroscopy was proved to be very valuable in analyzing the mechanism of co-agent-assisted peroxide vulcanization of EPM and EPDM [1–3]. Various examples of ^{13}C solid state NMR-based studies of EPDM networks can also be found in literature, investigating either sulfur [4,5] or peroxide crosslinking [6,7]. As far as resol crosslinking is concerned, few studies have been published, mostly relying on model systems [8]. Practically, resol cure is generally activated in order to achieve sufficiently high cure rates and degrees of crosslinking. This consists in introducing an acid species (e.g. stannous chloride, or an acid released by another chemical) that enhances cure rate via a carbo-cationic mechanism [9].

From an academic point of view, the chemistry of EPDM crosslinking is now understood satisfactorily, and the different mechanisms are summarized in Ref. [9]. However, the kinetics of EPDM crosslinking is usually studied with rheometers, and interpretation in terms of standard chemical reaction kinetics is therefore not straightforward. Moreover, the effects of the additives entering EPDM formulations (oil, fillers and other chemicals) on the crosslinking reaction are not yet characterized completely. However, proton NMR T_2 relaxation analysis of sulfur-vulcanized, oil-extended EPDM specimens very interestingly enabled several relationships to be established between sample composition, molecular mobility and the network density [10].

The traditional methods for analyzing rubber networks are equilibrium swelling measurements and viscoelastic or mechanical testing. The analysis of such properties has been practiced for long to demonstrate the existence of different network features and has supported the development of the first theoretical models like the affine [11] or the phantom network models [12]. In the former, the shear modulus is given by

$$G_e^{affine} = \nu RT = \frac{\rho RT}{\overline{M}_c} \quad (1)$$

where ν is the density of elastically active chains and $\overline{M}_c$ the average molar weight of these chains. An elastic chain is defined as a chain attached to the network at each of its two ends. For the phantom model, the junctions (crosslinking points) are free to fluctuate and the shear modulus is thus lower than in the case of the affine network.

$$G_e^{phantom} = (\nu - \mu)RT \quad (2)$$

where μ is the density of junctions.

The phenomenological model developed by Langley [13] and Dossin and Graessley [14] involves an additional term accounting for the topological contributions. According to the entanglement interpretation of the topological contributions, a portion of the restrictions on configurational rearrangements of macromolecules becomes permanently trapped when a network is formed and therefore is able to contribute to the equilibrium elasticity. The modulus can be expressed as

$$G_e^{Langley-Graessley} = (\nu - h\mu)RT + G_e^{max}T_e \quad (3)$$

where h is an empirical parameter between 0 and 1. T_e is the fraction of trapped entanglements in the network, i.e. the proportion of the maximum concentration of topological interactions that contributes to the modulus. G_e^{max} is the maximum topological contribution. It is expected to be very close to G_N^0, the plateau modulus of the un-crosslinked, high molar weight polymer. More recently, the slip-link model [15,16] refined the modeling of entanglements as slip-links joining polymer chains together and likely to act as additional crosslinks.

Discrepancies between theory and experiment still remain and the role of chain entanglements, network defects such as dangling chains, and network heterogeneities, is certainly a key issue. Ferry [17] suggested that the molecular mechanism responsible for the long-time relaxation process is the diffusion of dangling chain ends in the presence of entanglements. The contribution of the latter to the elastic modulus was illustrated for example by Patel et al. [18], by means of mechanical testing and equilibrium swelling measurements. These workers compared ''ideal'' polydimethylsiloxane networks (formed from pure difunctional PDMS, which yielded perfect networks without pendent chains) with imperfect ones having an equivalent value of ν but containing many pendent chains, created by using monofunctional PDMS mixed with the difunctional species. NMR can also be considered for characterizing the statistical structure of randomly crosslinked materials, as demonstrated for instance by Viallat et al. [19] who investigated the mechanisms of swelling and related changes of chain segment conformation in EVA/EMA gels in the presence of increasing concentrations of solvent.

Of course the viscoelastic behavior of vulcanizates has been investigated intensively in relation to their network features. The introduction of polymer dynamics concepts allowed some progress in the molecular theories developed for such vulcanizates. A molecular interpretation of the long-time relaxation of elastomers, based on the results by De Gennes [20] for the reptation of a single branched chain with topological constraints, was first given by Curro and Pincus [21]. Their model is based on the retraction of pendent chains in a crosslinked network with topological constraints (entanglements). It predicts that a polymer network containing a random distribution of dangling chain ends leads to a relaxation modulus having a power law dependence on time [21,22], as in the phenomenological Chasset and Thirion equation [23]. Indeed, Chasset and Thirion postulated in 1960s that an excellent representation of the isothermal relaxation modulus data for many rubbers can be given by

$$E(t) = E_\infty \left[1 + \left(\frac{t}{\tau_0}\right)^{-m}\right] \quad (4)$$

for long times t. E_∞ is the equilibrium modulus, and m and τ_0 are material parameters. So, Curro and co-workers provided an *a posteriori* theoretical background to this empirical equation and supported the conjecture of Ferry [11] that dangling chain ends lead to extremely long viscoelastic processes. Curro and Pincus theory predicts that the model parameter m is proportional to crosslink density, which was found to be in agreement with some experimental data on natural rubber. However, this point was discussed and criticized by McKenna and Gaylord [24]. In the following decade, end-linked elastomers like polydimethylsiloxanes were preferred for studying the terminal relaxation behavior of networks with dangling chains since, contrary to randomly crosslinked networks, the former allow to decouple the effect of crosslink density from that of the molar weight of pendent chains. This enabled some studies to focus on the dependence of the Chasset–Thirion exponent m with the molar mass and the distribution of molar masses of pendent chains or, for instance, with their number of entanglements [25,26]. Consistent trends were observed in both studies, showing that m is inversely related to the mass average molar mass of the pendent chains (and then, the number of entanglements per dangling chain).

As far as industrial development is concerned, the relaxation mechanisms in the long-time limit are of great importance because they define the elastic properties and creep behavior of crosslinked elastomers. Among numerous other experimental procedures, the compression set test is commonly carried out. It reflects the elastic recovery properties of elastomeric materials. However, through a viscoelastic analysis like that of Joubert et al. [27], who followed the molecular approach developed by Curro and co-workers [21,22], the results can be discussed on the basis of molecular mechanisms in the long relaxation times and can therefore be correlated to the structure of the crosslinked network. Indeed, in Joubert's paper, ethylene-vinyl acetate samples crosslinked by two methods could be clearly distinguished from the elastic recovery point of view with respect to their microstructure.

Upon literature overview, it is striking that, in the case of EPDM, viscoelastic analysis is not very much developed. Actually, despite its intensive use in industrial applications, EPDM is a complex polymer whose microstructure has often been said to contain ''microgels'', i.e. microcrystalline regions, which make rheological analysis even more critical. Therefore, the majority of studies devoted to it relies on NMR spectroscopy, as previously mentioned. This technique allows network density analysis in terms of chemical crosslinks as well as temporary and trapped entanglements. It is also possible with the T_2 relaxation method to estimate the amount of highly mobile chains, i.e. extractable material and network defects as dangling chains and chain loops. In the case of plasticized EPDM compounds, increasing oil content causes the decrease of entanglement density [10]. EPDM network density was shown to largely influence the mobility of oil molecules, which is more hindered as the network density is higher. These observations emphasize the interest of NMR spectroscopy as a complementary technique to rheology for the investigation of the structural characteristics of rubbery networks such as topology, heterogeneity (molar mass distribution of network chains) and amount of defects, which all could largely influence volume average chain dynamics and macroscopic properties.

Thus, the aims of the present paper are (i) to characterize the structure of oil-extended EPDM networks by performing classical physico-chemical and viscoelastic measurements in relation with relevant molecular models, in the purpose of (ii) analyzing the role of entanglements and dangling chain ends and (iii) modeling their long-time relaxation behavior to be able (iv) to predict compression set data from relaxation data.

2. Experimental

2.1. Materials

Experiments were carried out with EPDM Vistalon 8800 (ExxonMobil Chemical), in which the diene species is ethylidene norbornene (ENB). The following values of molar weight were measured: $\overline{M}_n = 160,000$ g/mol and $\overline{M}_w = 310,000$ g/mol. The molar content of each component in the terpolymer was assessed by ^{13}C NMR: 59.5 mol% ethylene, 38.3% propylene and 2.2% ENB. Vistalon 8800 actually comprises neat EPDM with a specific gravity of 0.86 g cm^{-3}, extended with 13% (w/w) paraffin oil. This results in a total specific gravity of 0.87 g cm^{-3} and a Mooney viscosity $ML_{(1+4)}$ of 73 at 125 °C. Additional paraffin oil (Torilis 7200, TotalFinaElf, France) was incorporated to Vistalon 8800 to mimic industrial compositions. The specific gravity of this plasticizer is 0.90 g cm^{-3} at 20 °C. Its proportion in the binary EPDM/plasticizer mixture was set to the industrial standard for most samples, i.e. 60 wt.% or phr (grams per hundred grams of Vistalon 8800). The corresponding volume fraction of plasticizer (initially present + added) is 0.44.

Radical crosslinking of EPDM was carried out by means of an octylphenol–formaldehyde resin (SP1045, Schenectady International, USA) called resol in the following. The reference amount of resol was 4% w/w (or phr) on EPDM basis and 0.6 phr $SnCl_2$ was used for crosslinking catalysis. In order to vary the degree of crosslinking from the standard formulation, the materials were prepared with diverse amounts of curing resin: 1, 1/4, 1/7, 1/10 and 1/30 of the reference quantities of resol, and an un-crosslinked sample was made for comparison (0 phr resol). All samples were prepared with a constant content of 0.6 phr of stannous chloride, $SnCl_2$. In the following, materials crosslinked with the regular amount of curing additives will be named ''reference'' samples (REF), whereas the others will be referred to via the corresponding ratio of crosslinking agent (RES0, RES1/4, RES1/30…).

The polymer and chemicals were kindly supplied by Hutchinson (Chalette-sur-Loing, France). They were used as-received from the supplier.

2.2. Sample preparation

The blends of the polymer, processing oil and curing system were prepared in an internal batch mixer (Haake Rheomix 600, Thermo Electron), at the temperature of 120 °C. The following protocol was adopted: first, the polymer was introduced (at time $t = 0$) into the cavity and sheared by itself for 5 min at 120 rpm in order to ensure thermal homogenization. The plasticizer was then poured in and the two components were mixed for the necessary time to reach torque stabilization. Before the introduction of the curing system, the temperature and rotation speed were decreased (80 °C and 50 rpm, respectively) and torque stabilization was waited for, again. The curing system (resin + catalyst) was then introduced and mixing was allowed to go on until torque started to increase. The blend was rapidly dumped in order to prevent the crosslinking reaction from occurring inside the mixer.

After dumping, test samples of every composition were compression moulded into 1-mm thick sheets for 5 min at 110 °C (no crosslinking occurred during this operation). Some of them were aimed at viscoelastic measurements for monitoring the crosslinking reaction at 200 °C, and assessing the reaction time and material thermal stability. Then, the other samples were crosslinked during molding in press at 200 °C for different times corresponding to the completion of reaction.

All samples were stored away from light at room temperature.

2.3. Measurements of the polymer soluble fraction

The total soluble weight fraction in the crosslinked samples was extracted with tetrahydrofuran using standard procedure, over 96 h with several renewals of the solvent. Since this soluble fraction includes all the plasticizers initially present in the sample, the soluble polymer weight fraction w_s could be expressed with respect to the mere sample polymer content, after subtraction of the plasticizer amount.

2.4. Viscoelastic measurements in oscillatory mode

All specimens (un-crosslinked and crosslinked) were tested in the form of 1-mm thick disks on a Rheometrics RMS800 rheometer under nitrogen atmosphere, using either 13 mm or 25 mm parallel plate geometry (depending on the torque level), in the linear viscoelastic regime. The extent of the linear viscoelastic domain was determined by means of strain sweeps as illustrated in Fig. 1. It can be noticed that the maximum strain for linear viscoelasticity is at least 20–30% for samples RES1/30, RES1/10 and RES1/7, whereas RES1/4 and REF exhibit non-linear behavior at strains exceeding ca. 10% and 1%, respectively. The evolution of the viscoelastic properties of the un-crosslinked polymer upon addition of plasticizer was examined in a previous paper [28] and is illustrated in Fig. 2.

The evolution of the dynamic moduli G' and G'' and of the loss tangent $\tan\delta$ during crosslinking of the polymer matrix was followed by time sweep oscillatory shear experiments

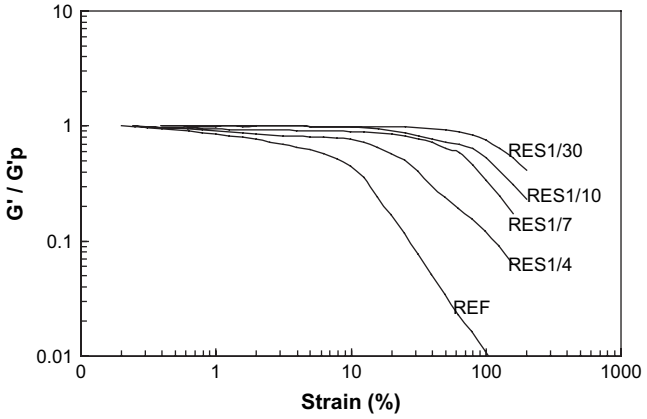

Fig. 1. Evolution of the normalized storage modulus G'/G'_p with shear strain (200 °C, 6.28 rad s^{-1}). G'_p is the low-strain plateau modulus.

($\omega = 6.28$ rad s^{-1}) at 200 °C. The time at which no further significant variation of the moduli occurred was considered as the time necessary for the chemical reaction to be completed and therefore determined the duration of the molding operation for the samples to be cured directly after being dumped from the batch mixer. At the end of each of the time sweep experiments, a frequency sweep was performed in order to characterize the network formed. The value of the equilibrium modulus G_e was determined from the low frequency plateau exhibited on G' plots.

2.5. Long-time relaxation measurements and compression set tests

Cured samples were submitted to a compression set test, with a dynamic mechanical analyzer (DMA 2980, TA Instruments, USA) allowing relaxation experiments, according to the following protocol. A 4-mm diameter, 1.3-mm high cylindrical sample was placed between the plates and submitted to a compression strain of 25% for 10 h (sample initial height and deformation were controlled very precisely on the apparatus), while recording the stress relaxation. At the end of this time, the stress was instantaneously removed, allowing for strain

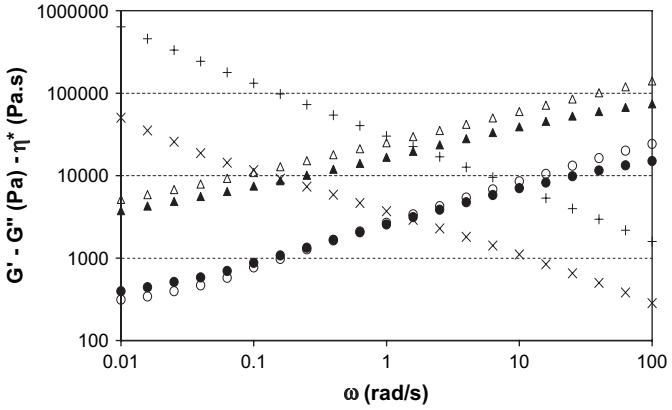

Fig. 2. Viscoelastic behavior of un-crosslinked EPDM in the linear domain at 200 °C: G' (open symbols), G'' (closed symbols) and η^* (crosses). △, ▲ and +: non-plasticized EPDM Vistalon 8800. ○, ● and ×: EPDM Vistalon 8800 plasticized with 60 phr oil (volume fraction of EPDM: $\phi = 0.56$).

recovery, which was monitored for another 10 h. The test temperature was 100 °C. It must be reminded that under 25% strain, all the samples except for REF and RES1/4 remained within their linear viscoelastic domain.

3. Modeling of the elastic modulus of the networks

It must be noted that Eqs. (1)–(3) were developed for "dry" networks and have to be modified for networks which contain a soluble species acting as a diluent. The expression for the modulus of the "dry" network after extraction is similar to the one derived by Flory [11] for a network swollen in a solvent, and can be written as

$$G_e/RT = (\nu - \mu)(1 - u_{sol})^{1/3} \tag{5}$$

for a phantom network. u_{sol} is the volume fraction of the soluble species. As mentioned previously, the characteristics of the networks were derived from the experimental determinations of the equilibrium modulus G_e and the soluble fraction. We consider the phenomenological model developed by Langley, Dossin and Graessley, as presented in Eq. (3). Values of ν, μ and T_e can be calculated from the polymer sol fraction w_{sol} as will be explained later. However, our EPDM networks also contain large amount of plasticizer and are thus swollen by this extractable component which acts as a diluent. In order to take this into account, corrections are introduced for the plasticizer into both contributions to the modulus. Consequently, on the one hand, the network contribution $(\nu - h\mu)$ RT must be corrected by $\theta^{1/3}$, where θ is the polymer volume fraction of the compound, analogous to $(1 - u_{sol})$ in Eq. (5). On the other hand, the entanglement contribution is also altered by the presence of oil and in that case the effect is that of a diluent in an entangled, un-crosslinked polymer. This point was addressed in a previous paper [28]. The terminal viscoelastic parameters of this EPDM in the presence of the same plasticizer were derived from the bulk polymer ones with a correction based on the free volume theory. This correction is of the form $\theta^{2.25}$, as shown with different polymer systems [29,30], which is in agreement with the founding theoretical work by Daoud et al. [31].

Finally, the shear modulus of the network in the presence of a plasticizer can be written as

$$G_e = (\nu - h\mu)RT\theta^{1/3} + G_e^{max}T_e\theta^{2.25} \tag{6}$$

The parameters ν, μ and T_e can be calculated using the theoretical relations established by Pearson and Graessley [32,33], as described hereafter. In our case, the soluble polymer fraction, w_s, has been measured. From this knowledge, the extent of reaction p (=fraction of crosslinkable moieties effectively involved in crosslinks) can be computed from the following equation:

$$p = b\left(w_s^{-1/(b+1)} - 1\right)/(r_n\xi) \tag{7}$$

with $\xi = (1 - w_s)$ and $b = r_n/(r_w - r_n)$, where r_n and r_w are the number average and weight average of crosslinkable reactive sites, respectively.

A randomly chosen un-crosslinked polymer unit is connected to the network in either of the following manners: it can be connected to the gel along only one of the two paths leading away from it (probability ψ_1) or along both paths (probability ψ_2).

The probability ψ_2 can be computed as follows:

$$\psi_2 = 1 - 2\varepsilon + (1 + pr_n\xi/b)^{-b-1} \tag{8}$$

where

$$\varepsilon = \left[1 - (1 + pr_n\xi/b)^{-b}\right] \Big/ pr_n\xi \tag{9}$$

and then

$$\psi_1 = 2(1 - \varepsilon - \psi_2) \tag{10}$$

Finally, ν, μ and T_e are available through

$$\nu = \frac{\rho}{2M_0}p\left[3\psi_1\psi_2 + 2\psi_2^2\right] \tag{11}$$

$$\mu = \frac{\rho}{2M_0}p\left[2\psi_1\psi_2 + \psi_2^2\right] \tag{12}$$

$$T_e = \psi_2^2 \tag{13}$$

where M_0 is the molar weight of the molecular segment between two consecutive reactive sites, i.e. between two ENB moieties. The following value was obtained from the ENB % and from the molar weight of the terpolymer: $M_0 = 1520$ g/mol. r_n and r_w could then be derived: $r_n = \overline{M}_n/M_0$ and $r_w = \overline{M}_w/M_0$.

4. Modeling of the viscoelastic properties in the long-time range: relaxation and strain recovery

Although of real interest from an industrial point of view, the compression set property is scarcely addressed on real systems from a computational point of view. However, it can be treated in a viscoelastic framework as demonstrated by Joubert et al. [27]. Here, we performed similar calculations based on the relaxation data. It must be noted that the development of a constitutive model is beyond the scope of the present paper; therefore the equations implemented for modeling the stress and strain response of our materials were taken from linear viscoelastic theory. It is clear that, as mentioned in Section 2.5, this is only an approximation for samples RES1/4 and REF. This will be considered in the discussion of the results (see Section 5.4). The computational method is described below.

As mentioned in Section 1, the Chasset–Thirion equation (Eq. (4)) can be used quite satisfactorily to model the relaxation modulus of rubbers in the long-time range. So, we determined for each sample the values of the three Chasset–Thirion parameters (E_∞, τ_0 and m) by fitting the experimental data from the relaxation stage of the compression set test. The time range over which the fit was performed was taken between 10 min (Chasset–Thirion model is *a priori* not well suited for short times)

and 600 min (beginning of the strain recovery stage). However, it was noticed that, in most cases, the fit remained very satisfactory below 10 min.

Fitting this data by a mathematical equation enabled us to extrapolate the modulus evolution to times longer than 600 min, which was made necessary for the strain recovery modeling. Indeed, in order to calculate the evolution of the residual strain over the 10 h following the suppression of the stress, the creep compliance had to be known over the same time interval. It was derived from the relaxation modulus by solving the integral convolution equation relating the relaxation modulus $E(t)$ and the creep compliance $J(t)$ in linear viscoelasticity:

$$t = \int_0^t E(u)J(t-u)\mathrm{d}u \tag{14}$$

following the stepwise numerical method based on trapezoid approximation described in Ref. [34]. Then, once $E(t)$ and $J(t)$ were determined over the whole time domain (0–1200 min), the Boltzmann superposition principle was used to derive the evolution of strain as follows:

$$\varepsilon(t) = \int_{-\infty}^{t} \frac{\mathrm{d}\sigma(u)}{\mathrm{d}u} J(t-u)\mathrm{d}u \tag{15}$$

where σ is the stress. $\sigma(t) = \varepsilon_0$. $E(t)$ for $t < t'$ ($t' = 600$ min) and $\sigma(t) = 0$ for $t < t'$.

So,

$$\underset{t>t'}{\varepsilon(t)} = J(t)\sigma(0) + \int_0^{t'} \frac{\mathrm{d}\sigma(u)}{\mathrm{d}u} J(t-u)\mathrm{d}u + \int_{t'}^{t} \frac{\mathrm{d}\sigma(u)}{\mathrm{d}u} J(t-u)\mathrm{d}u \tag{16}$$

which yields, after integration by parts and rearrangement:

$$\frac{\varepsilon(t)_{t>t'}}{\varepsilon_0} = J(t)E(0) + \int_0^{t'} \frac{\mathrm{d}E(u)}{\mathrm{d}u} J(t-u)\mathrm{d}u - E(t')J(t-t') \tag{17}$$

The evolution of the residual strain, and thus of the compression set, can then be calculated over the whole recovery stage of the compression set experiment, i.e. from time $t' = 600$ min to 1200 min. From a practical point of view, the calculations were performed with the Mathcad7® software (Mathsoft Inc./Parametric Technology Corp., USA).

5. Results and discussion

5.1. Viscoelastic properties of the crosslinked samples at 200 °C

The temperature chosen for crosslinking was 200 °C and only the influence of resol amount on viscoelastic properties was studied in the parallel plate rheometer. Fig. 3 exhibits

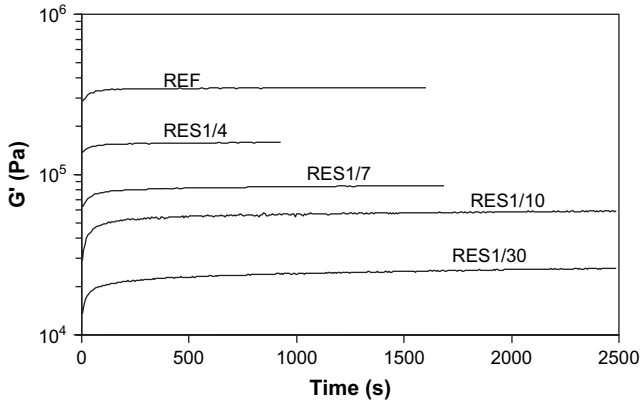

Fig. 3. Evolution of G' with time for the samples during crosslinking (200 °C, 6.28 rad s^{-1}, linear viscoelastic domain).

the evolution of the storage modulus G' with time for all samples containing the crosslinking agent. All recordings exhibit a plateau at long times which expresses the complete reaction and thermal stability. The very beginning of the crosslinking reaction is difficult to capture because it starts as soon as the specimen is placed between the rheometer plates until it reaches the set temperature. Nevertheless, it is clear that the time needed by the modulus to reach a plateau gets longer as resol concentration is lower. It can be seen that the modulus regularly increases as resol input is increased. The frequency sweeps performed after reaction completion yielded the low frequency G' (and so G_e) and tan δ values reported in Table 1. Improvement of the "perfect" nature of the network can be inferred from the decreasing tendency of tan δ when the amount of curing system increases, as a consequence of the enhancement of the degree of crosslinking (shortening of the elastic chains between crosslinks). A quasi-linear relationship can be noticed between G_e and resol concentration, which supports the conclusion that the crosslinking agent efficiency does not depend upon its concentration.

5.2. Determination of the network characteristics according to Pearson and Graessley's approach

As explained in Section 3, the known density of crosslinkable sites on the polymer backbone (yielding r_n and r_w) and the measured soluble polymer fraction in the formed network (oil subtracted) w_s, enabled us to derive all the structural parameters which, within the framework of Pearson and Graessley's theoretical approach of randomly crosslinked

Table 1
Linear viscoelastic parameters of EPDM networks crosslinked at 200 °C with different proportions of resol. Oscillatory measurements were carried out at 200 °C

Resol proportions (with respect to reference)	tan δ	G_e (Pa)
1	0.01	3.3×10^5
1/4	0.07	9.8×10^4
1/7	0.12	5.8×10^4
1/10	0.18	3.4×10^4
1/30	0.40	2.0×10^3

Table 2
Structural parameters for the different specimen, as computed from the theoretical relations derived by Pearson and Graessley [33]

Specimen	w_s[a]	p	ψ_1	ψ_2	ν[a] (mol m^{-3})	T_e	ν/μ	p' = nb of crosslinks/nb of diene moieties	h
REF	0.002	0.229	0.08	0.92	124	0.85	1.93	0.122	0.62
RES1/4	0.011	0.080	0.20	0.79	39	0.63	1.84	0.040	0.59
RES1/7	0.038	0.041	0.32	0.65	17	0.42	1.75	0.018	0.56
RES1/10	0.104	0.023	0.44	0.46	6.5	0.21	1.67	0.007	0.53
RES1/30	0.300	0.012	0.50	0.20	1.25	0.04	1.58	0.002	0.51

[a] Expressed with respect to volume of polymer without taking plasticizer into account.

tetrafunctional networks, reflect the evolution of the structure when increasing the concentration of the curing agent. Table 2 presents the values of w_s, from which p, ψ_1 and ψ_2 are computed. The network characteristics ν, T_e, ν/μ and the empirical parameter h from Langley and Graessley's model are then derived. The value of the ratio between the number of chemical crosslinks, and the number of diene moieties (i.e. of reactive sites) available in the volume considered, called p', is also given for comparison purposes with p. The determination of p' required to calculate the concentration of crosslinkable sites (i.e. ENB moieties). This concentration could be derived from the knowledge of the ENB content of the terpolymer. This also allowed to calculate the average molar weight of the chain segments between two consecutive reactive sites, M_0, involved in Eq. (12). So, on the one hand, p is obtained from a theoretical background relying only on the knowledge of the soluble polymer fraction. On the other hand, p' is derived from the whole computation originating from p and therefore allows a cross-checking of the results concerning the chemical network.

Fig. 4 displays the evolutions of the major structural parameters, namely ν, T_e, ψ_1 and ψ_2, with the increasing concentration of resol used (expressed in phr). Logically, the crosslink density ν and the proportion of trapped entanglements T_e, which is linked to the probability ψ_2, increase with the resol fraction. Simultaneously, the probability of forming dangling chains decreases. In contrast with ν, which follows an almost linear evolution with the crosslinking agent fraction, T_e exhibits a dramatic increase at low resol fractions, and a much

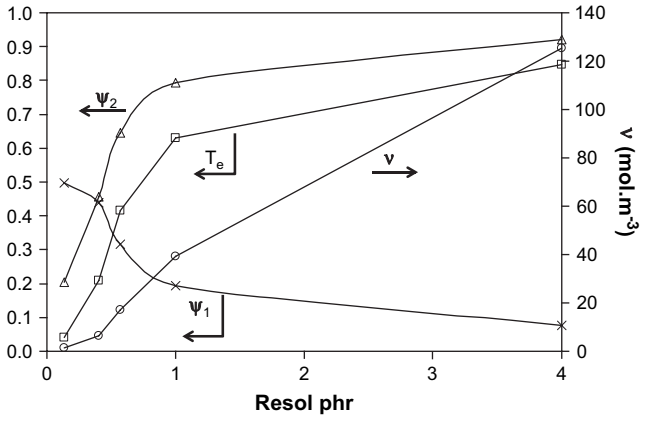

Fig. 4. Evolution of the network structural features with the proportion of crosslinking agent. The computed parameters are ν (○) and T_e (□) from Langley and Graessley model (Eq. (3)), derived from ψ_1 (×) and ψ_2 (△), as introduced by Pearson and Graessley (Eqs. (8)–(13)).

slower increase above 1 phr resol. This was expectable, considering that from a certain network density, the long range chain mobility is highly hindered (60% of trapped entanglements) and then the possibility for a chain to "escape" from getting crosslinked to others largely decreases.

Table 2 shows that the ν/μ ratio increases with increasing the curing agent concentration and tends towards 2, which is the theoretical value for tetrafunctional network. This is an indication of the network evolving towards a more and more "perfect" structure when increasing crosslink density and concomitantly decreasing dangling chain occurrence (ψ_1). This evolution towards a tetrafunctional network containing supposedly less defects is supported by the comparison of p' and p: indeed, it can be seen that the ratio p'/p gets nearer to 0.5 as resol phr increases. For an ideal tetrafunctional network, p' should be strictly equal to $p/2$, since one chemical crosslink involves two norbornene moieties. Here, the matching of p' with $p/2$ improves for samples closer to reference.

The last column in Table 2 presents the values of the empirical parameter h, whose determination was carried out as follows. Considering Eq. (6), it can be seen that plotting the values of G_e/T_e vs. $(\nu RT)/T_e$ should yield a straight line whose slope and intercept are $(1-(h\mu/\nu))\theta^{1/3}$ and $G_N^0\theta^{2.25}$, respectively. Actually, we performed a linear regression over the values, after discarding those for sample RES1/30 which were out of range, and obtained a slope of 0.56 (correlation coefficient $R^2 = 0.94$). This enabled us to compute h for each sample (from experimental G_e). It can be noticed that h increases with resol fraction. As mentioned by Pearson and Graessley, h is difficult to establish theoretically, but it should be near 1 for highly entangled networks. So our results are consistent with this statement, and show, as could be expected, that the higher the crosslinking density, the higher the entanglement density, due particularly to entanglement trapping.

At the same time as the slope, the intercept was calculated, yielding a numerical value of G_N^0 for the non-plasticized polymer, which could not be measured from rheological tests on un-crosslinked materials. Here, $G_N^0 = 2.1\times10^5$ Pa, and $G_N^0\theta^{2.25} = 5.7\times10^4$ Pa, which would represent the plateau modulus of the plasticized material. Considering the shapes of the plots in Fig. 2, these values are quite realistic, but it must be noted that for such a platicized polymer, if a plateau existed, it would probably occur at very high frequencies.

Now, the whole set of Langley and Graessley's model parameters was available for recalculation of the equilibrium modulus, $G_{e\ calc}$ according to Eq. (6). The correlation of G_e and $G_{e\ calc}$ is reported in Fig. 5. Very satisfactory agreement

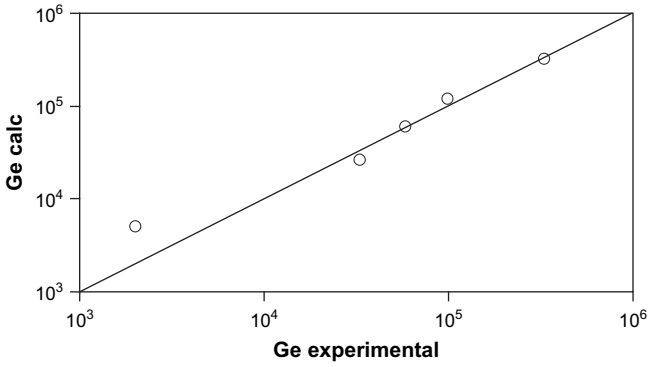

Fig. 5. Comparison of computed shear equilibrium modulus (Eq. (6)) and experimental data at 200 °C.

can be observed (slope of the regression is 0.97 and $R^2 = 0.99$), which validates our approach that relies on a rubber network theory expressing the topological contributions from the permanently entangled chains, and also refers to another theoretical background based on the free volume concept to account for the diluting effect of the plasticizer. However, it must be noted that the effect of the concentration of the latter is not addressed in the present work, although it is likely to be of great influence towards the crosslinking kinetics, due to the modified polymer chain mobility, and so presumably towards network structure.

5.3. Long-time relaxation behavior at 100 °C

As mentioned in Section 1, network defects have long been shown to mainly affect the long-time behavior of rubber vulcanizates. In evaluating our samples for elastic recovery after prolonged strain at 100 °C, the compression stage of the test was analyzed from the viscoelastic point of view, since it corresponds to conditions of relaxation under constant strain over 10 h.

The recordings of the modulus of the different samples are plotted in Fig. 6. It is apparent that these relaxation curves are not positioned in the same manner as those for G_e with respect to resol concentration. Whereas G_e was evolving quasi-linearly with the latter, the relaxation plots of the least crosslinked material (RES1/30) exhibits a different pattern from the

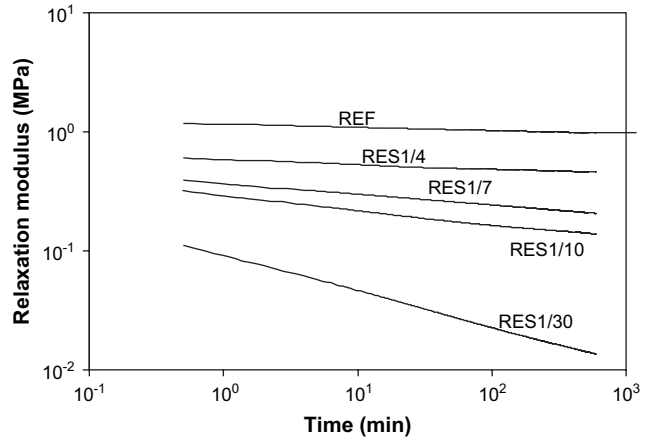

Fig. 6. Evolution of the relaxation modulus measured over 10 h at 100 °C, under 0.25 compressive strain.

Table 3
Fitted parameters of Chasset–Thirion equation for the shear stress relaxation of plasticized EPDM networks (strain = −0.25)

Specimen	E_∞ (Pa)	τ_0 (min)	m
REF	6.3×10^5	0.09	0.067
RES1/4	2.6×10^5	13	0.070
RES1/7	1.2×10^5	104	0.170
RES1/10	7.0×10^4	512	0.184
RES1/30	4.0×10^3	8000	0.348

others. For quantitative comparison purposes, the data were fitted with Chasset and Thirion equation, so that E_∞, τ_0 and m were determined for each specimen. These values are reported in Table 3.

Interestingly, the orders of magnitude of E_∞ follow a significant evolution. The equilibrium relaxation modulus of sample RES1/30 is clearly out of the range of the others. This has of course to be related with the presence of un-crosslinked chains (cf. w_s) and with the amount of dangling chains (cf. ψ_1). Although it gets slower as the dangling chains are longer, the relaxation is possible and the modulus keeps on decreasing consequently towards very low values of E_∞. The higher crosslink density and trapping factor of REF and RES1/4 are responsible for moduli which remain over 2×10^5 Pa, i.e. much higher than the level of the estimated plateau modulus of the un-crosslinked plasticized polymer.

The characteristic relaxation times τ_0 are worth paying some attention too, although their magnitude cannot be compared with published data for similar systems. Only their evolution between the different samples can be commented. Again, this evolution is very consistent with the supposed role of the dangling chains. The extreme values of τ_0 are about five decades apart. As shown in the works by Curro and Pincus, which refer to natural rubber with zero soluble fraction, the relaxation of a dangling chain (i.e. a chain linked to the network by only one of its extremities) is assimilated to the reptation of star-like molecules, whose relaxation times evolve exponentially with their molar mass. So, from a qualitative point of view, our results demonstrate that for imperfect networks such as our low crosslinked samples, the long-time relaxation mechanisms are largely emphasized, supposedly due to the presence of long dangling chain ends.

The exponent m from Chasset–Thirion equation cannot be compared to published data neither, and the analysis of the crosslink dependence of m cannot be carried out with the Curro and Pincus approach. Indeed, the decrease of m when resol quantity is increased, which is observed in the present study, is opposite to the proportional relation derived by these authors in their theory. The major reason for this discrepancy is certainly that our networks, which contain both plasticizer and soluble polymer fractions, do not fit into the assumptions of the Curro and Pincus theory.

5.4. Compression set at 100 °C

The relaxation experiments described above were followed by a 10 h recovery stage, during which the evolution of strain

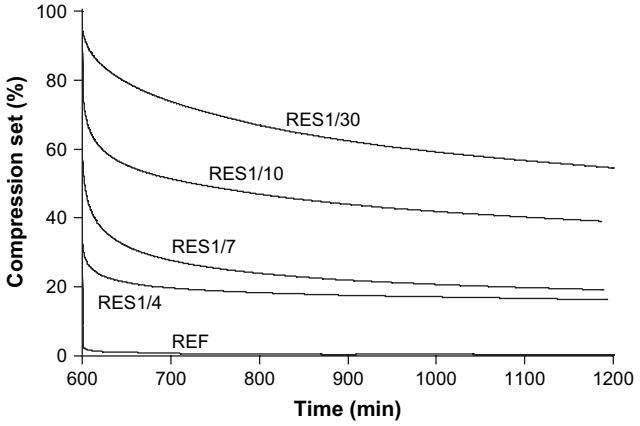

Fig. 7. Evolution of the compression set (i.e. (residual strain/initial strain)%) during strain recovery monitored at 100 °C, over 10 h after release of the compressive stress at $t = 600$ min.

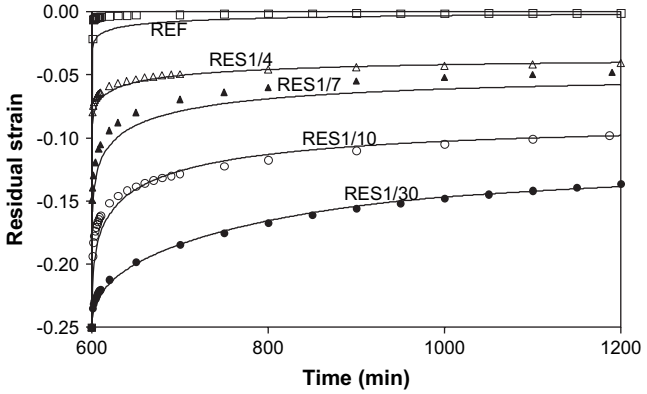

Fig. 8. Comparison between residual strain computed from Eq. (17) and measured data during recovery at 100 °C. Symbols: experimental; solid lines: model.

was continuously recorded. The experimental data, expressed in terms of compression set (i.e. % of residual strain) and residual strain, are reported in Fig. 7 and in Table 4 for the different materials. It is shown that only the reference material has an almost 0% residual strain after 10 h of recovery. All other materials are still evolving after 10 h, and no stable state is reached. Obviously, compression set is small when the crosslink density is high and the network free of defects. Consequently, the results concerning samples RES1/10 and RES1/30 consist in compression sets of around 40% and over, which correspond to total residual strains above 10%. The bad performance of these materials is certainly to be linked to un-crosslinked chains and to network defects such as long dangling chains, which do not contribute to the permanent network and are able to relax during the compression stage, then providing no elastic contribution during the recovery stage.

The results of the compression set modeling are illustrated in Fig. 8 through the evolution of residual strain in time, the final values being given in Table 4. It is clear that the model is able to capture the general trends of the materials' recovery behavior. Slight discrepancies are observed, which certainly originate from different factors depending on the specimen, although of course the principle itself of the computation contains several approximations and sources of error which can affect all samples: the fitting of the experimental data of modulus and extrapolation, the trapezoid approximation in the creep compliance calculation, the numerical resolution of the integral term in Eq. (17), etc.

Table 4
Compression set and residual strain after 10 h compression at constant strain (−0.25), followed by 10 h recovery, at 100 °C

Specimen	Experimental		Modelled strain (−)
	Compression set (%)	Strain (−)	
REF	0.4	0.001	0.002
RES1/4	16.3	0.041	0.040
RES1/7	19.2	0.048	0.058
RES1/10	39.1	0.097	0.098
RES1/30	54.6	0.137	0.140

More specific points can be discussed. As far as the reference sample is concerned, the nominal strain applied (−0.25) was mentioned to be out of the linear viscoelasticity range, which is most likely to explain the underprediction of the model. However, even for those samples which remained in their linear domain, the model underpredicts the strain at the beginning of the recovery process. In this case, the reason is more likely to be the lack of accuracy on the modulus values at the very first instants of relaxation. Indeed, during the relaxation test, firstly the strain could obviously not be applied strictly instantaneously, and secondly, the data acquisition started after some delay. The consequence is that the value of the initial modulus, $E(t = 0)$ had to be somewhat extrapolated. Computations for the first instants of recovery have been observed to be sensitive to experimental error on $E(t = 0)$. On the other hand, some extrapolation was also necessary at long times, from 600 min to 1200 min, for recovery modeling purposes. This extrapolation was provided by fitting the data with the Chasset–Thirion model which obviously can induce some inaccuracy and affect the quality of the results in the long-time range. This is probably what can be noticed on the plot corresponding to the RES1/7 sample.

Nevertheless, it can be concluded that the compression set test can be predicted from the mere knowledge of the material relaxation behavior. The agreement with experimental data is satisfactory. These results are quite original in the field of industrial compounds such as, among others, plasticized EPDM networks.

6. Conclusions

Plasticized EPDM compounds were crosslinked by means of octylphenol–formaldehyde resin (resol) whose concentration was adjusted by a factor up to 1/30 in order to induce large variations of the crosslink density. A significant increase of the soluble polymer weight fraction was observed along with the decrease of the crosslink density. Viscoelastic measurements in oscillatory mode were carried out in order to determine the equilibrium modulus G_e and to support a characterization of the network features based upon the

phenomenological model of Langley and Graessley whose parameters are ν, the concentration of active chains, μ, the concentration of junctions and T_e, the fraction of entanglements trapped when the network was formed. The knowledge of the polymer molecular characteristics and the soluble fraction in the different samples allowed the determination of the extent of reaction and of the probabilities for an un-crosslinked polymer unit to be linked to the network by only one or two paths. The former case corresponded to pendent chains. Then, ν, μ and T_e could be calculated. This provided a complete characterization of the networks, showing that the lower the crosslinking agent concentration, the higher the trapping factor, the more numerous and the longer the pendent chains. Such chains have long been known to be responsible for long-time relaxation mechanisms in elastomeric networks, according to considerations based on the reptation theory. Therefore, relaxation experiments were performed over long times, followed by elastic recovery monitoring. By fitting the relaxation data with the Chasset–Thirion equation, its parameters could be computed, especially τ_0, the characteristic time for the longest relaxation mechanisms. A dramatic increase was observed in τ_0 as the resol concentration decreased. This is another evidence of the presence of long dangling chains, which leads to very poor recovery properties of samples having low crosslink densities.

With these results, the aims of the present study were reached insofar as, from common physico-chemical and viscoelastic characterizations, several network parameters were quantified, and the role of entanglements and dangling chains could be proved through some features of the viscoelastic response of these networks. In addition, predictions of the compression set data were made possible by using the Chasset–Thirion equation to model and extrapolate the relaxation data in time. A very satisfactory agreement could be achieved between calculations and experiments. The method adopted here is somewhat original since it provides some theoretical background to the interpretation and prediction of an engineering property.

Acknowledgment

The authors gratefully acknowledge the Hutchinson Company (Chalette-sur-Loing, France) for making this work possible.

References

[1] Dikland HG, Van der Does L, Bantjes A. Rubber Chem Technol 1993;66:196.
[2] Dikland HG, Hulskotte RJM, Van der Does L, Bantjes A. Kautsch Gummi Kunst 1993;46:608.
[3] Murgić Z, Jelenčić J, Murgić L. Polym Eng Sci 1998;38:689.
[4] Litvinov VM, Van Duin M. Kautsch Gummi Kunst 2002;55:460.
[5] Winters R, Heinen W, Verbruggen MAL, Lugtenburg J, Van Duin M, de Groot HJM. Macromolecules 2002;35:1958.
[6] Palmas P, Le Campion L, Bourgeoisat C, Martel L. Polymer 2001; 42:7675.
[7] Orza RA, Magusin PCM, Litvinov VM, Van Duin M, Michels MAJ. Macromol Symp 2005;230:144.
[8] Van Duin M. Rubber Chem Technol 2000;73:706.
[9] Van Duin M. Kautsch Gummi Kunst 2002;55:150.
[10] Litvinov VM. Macromolecules 2006;39:8727.
[11] Flory PJ. Principles of polymer chemistry. Ithaca, NY: Cornell University Press; 1953.
[12] James HM, Guth E. J Chem Phys 1943;11:455.
[13] Langley NR. Macromolecules 1968;1:368.
[14] Dossin LM, Graessley WW. Macromolecules 1979;12:123.
[15] Ball RC, Doi M, Edwards SF, Warner M. Polymer 1981;22:1010.
[16] Edwards SF, Vilgis T. Polymer 1986;27:483.
[17] Ferry JD. Viscoelastic properties of polymers. 3rd ed. New York: Wiley; 1980 [chapter 10].
[18] Patel SK, Malone S, Cohen C, Gillmor JR, Colby RH. Macromolecules 1992;25:5241.
[19] Viallat A, Cohen-Addad JP, Cassagnau P, Michel A. Polymer 1996; 37:555.
[20] De Gennes PG. Scaling concepts in polymer physics. Ithaca, NY: Cornell University Press; 1979.
[21] Curro JG, Pincus P. Macromolecules 1983;16:559.
[22] Curro JG, Pearson DS, Helfand E. Macromolecules 1985;18:1157.
[23] Chasset R, Thirion P. In: Prins JA, editor. Proceedings of the conference on physics of non-crystalline solids. Amsterdam: North Holland; 1965. p. 345.
[24] McKenna GB, Gaylord RJ. Polymer 1988;29:2027.
[25] Vega DA, Villar MA, Alessandrini JL, Valles EM. Macromolecules 2001; 34:4591.
[26] Batra A, Cohen C, Archer L. Macromolecules 2005;38:7174.
[27] Joubert C, Michel A, Choplin L, Cassagnau P. J Polym Sci Part B Polym Phys 2003;41:1779.
[28] Ponsard-Fillette M, Barrès C, Cassagnau P. Polymer 2005;46:10256.
[29] Marin G, Menezes E, Raju VR, Graessley WW. Rheol Acta 1980; 19:462.
[30] Gimenez J, Cassagnau P, Michel A. J Rheol 2000;44:527.
[31] Daoud M, Cotton JP, Farnoux B, Jannink G, Sarma G, Benoit H, et al. Macromolecules 1975;8:804.
[32] Pearson DS, Graessley WW. Macromolecules 1978;11:528.
[33] Pearson DS, Graessley WW. Macromolecules 1980;13:1001.
[34] Hopkins IL, Hamming RW. J Appl Phys 1957;28:906.